MULTICHANNEL COMPRESSED SENSING VIA SOURCE SEPARATION FOR HYPERSPECTRAL IMAGES

Mohammad Golbabaee, Simon Arberet and Pierre Vandergheynst

Signal Processing Institute, Ecole Polytechnique Fédérale de Lausanne (EPFL), Switzerland
E-mail:{mohammad.golbabaei, simon.arberet, pierre.vandergheynst}@epfl.ch

ABSTRACT

This paper describes a novel framework for compressive sampling of multichannel signals that are highly correlated across the channels. In this work, we assume few number of independent sources are generating the multichannel observations based on a linear mixture model. Moreover, sources are assumed to have sparse/compressible representations in some orthonormal basis. The main contribution of this paper lies in rephrasing the compressed sampling of multichannel data as the compressive source separation problem by knowing the mixture parameters. A number of simulations measure the performance of our recovery algorithm. Comparing to the classical CS scheme -which recovers data of all channels separately- ours indicates a significant reduction in both, the number of measurements to be sent and the complexity of the decoding algorithm (i.e., scaling by the number of sources rather than the number of channels). We demonstrate an application of our scheme in acquisition of the Hyperspectral images. Our algorithm proposes an accurate, low cost and fast recovery from small number of the transmitted measurements that are taken by a low resolution camera.

Index Terms— Compressed sensing, Hyperspectral images, Mixture model, Source separation, Sparsity, l_1-minimization.

1. INTRODUCTION

Hyperspectral images (HSI) are a collection of hundreds of images which have been acquired simultaneously in narrow and adjacent spectral bands. HSI finds many applications including agriculture, mineral exploration and environmental monitoring. HSI are produced by *imaging spectrometers* which measure the light reflected from many areas, each of which represented as a pixel, on the Earth's surface. A prism splits the light into many narrow, adjacent wavelength and the energy in each band is measured by a separate detector. The spectral range and the spatial resolution of the HSI are restricted by limitations of detector designs, the requirements of data storage, transmission and processing [1].

As an alternative to the Shannon/Nyquist sampling which takes N periodic samples to acquire the data $x \in \mathbb{R}^N$, it is possible with the *compressive sampling* (CS) [2, 3] approach, to reduce the number of the measurements to $M < N$, if the data x has a sparse or compressible representation $\theta \in \mathbb{R}^N$ in some basis $\Psi \in \mathbb{R}^{N \times N}$ (i.e. $x = \Psi \theta$). CS measurements are inner product between a measurement vector, which can be a random vector, and the data vector x.

Thus, the set of measurements can be expressed in a matrix form

$$y = \Phi x \qquad (1)$$

where $y \in \mathbb{R}^M$ is the vector containing the CS measurements and Φ is the measurement matrix of size $M \times N$. The number of measurements M necessary for CS recovery is determined by the sparsity of x and the *mutual coherence* between the measurement matrix Φ and the basis Ψ, see [2, 3].

As it is costly to acquire each pixel of the HSI, it becomes very interesting to use the CS approach to acquire HSI. This can be done using the single-pixel hyperspectral camera (SPHC) [4], where the hyperspectral lightfield is focused onto a digital micromirror device (DMD). The DMD acts as an optical spatial modulator and reflects part of the incident lightfield into a spectrometer. Thus the DMD computes in the analog domain an inner product between a measurement vector with 0/1 entries, and the image in all the spectral bands simultaneously. As a consequence the same measurement matrix is applied to each spectral band image and each measurement depends on only one spectral band image. Different approaches to reconstruct the data form these separate measurements have been studied in [5].

In multichannel signals, the idea of exploiting the correlations across the channels have been studied in [6, 7] to decrease even more the number of the compressive measurements. These approaches assume the signals of all channels having more or less the same support. As a result only few measurements are required to recover the joint support, however, they are not sufficient to reconstruct the coefficients, which remains as the bottleneck of these schemes. In this paper we assume that the data is generated from a linear *source mixture* model, presented in section 2.1. We then propose a new sampling and transmission scheme for HSI in section 2.2 as well as a recovery algorithm in section 3. Simulations in section 4 show that we can drastically reduce the number of measurement needed to reconstruct the data as compared to the classical CS approach.

2. PROBLEM SETUP

2.1. Observations Model

In order to represent the hyperspectral images, define a matrix $X \in \mathbb{R}^{J \times N}$, where each of its rows X^j (in this note, by superscript we index a row of a matrix) corresponds to a slice of the global cubic image i.e, a 2-D image observed in a certain spectral band (we reshape this slice into an N dimensional vector). Here, J is the number of the spectral channels and N denotes the resolution of the images for each channel.

Typically there is a high dependency between the slice images of HSI (rows of X) i.e., the structures in the images are more or less preserved across the spectral channels, however some parts highlight

more or less in certain frequency ranges. This comes from the fact of having few subregions consisting of different materials and therefore due to their different frequency responses they reflect the light with specific attenuation across the frequency bands. We refer to these regions as different sources. More precisely, we define a source image $S^i \in [0, 1]^{1 \times N}$ as a positive valued vector which represents the percentage of a given material (indexed by i) in each pixel of the scene. As a consequence, for a given pixel of the scene (indexed by n), the sum of the consisting sources must be equal to one i.e., $\forall n \in \{1, ..., N\}$ the source images must satisfy $\sum_i S^i(n) = 1$. In practice, if the spatial resolution of the image is high compared to the structural content of the image, each pixel corresponds to only one material, which means that the sources are disjoint and take their values in the set $\{0, 1\}^{1 \times N}$. Moreover, for each source i there is a spectral response vector $A_i \in \mathbb{R}^{J \times 1}$ that is associated with each nonzero element of S^i. With descriptions above, any hyperspectral image can be decomposed by several distinct sources as following [1]:

$$X = AS. \tag{2}$$

Where, rows of the matrix $S \in \mathbb{R}^{I \times N}$ and the columns of $A \in \mathbb{R}^{J \times I}$ are collections of I source images and their corresponding spectral vector. If we assume the observed region is composed of few number of materials, say I^*, there will be only I^* rows in S which have nonzero energy and hence, (2) can be rewritten as,

$$X = A_{\mathcal{I}^*} S_{\mathcal{I}^*}, \tag{3}$$

where, $\mathcal{I}^*$ is the set that indexes the active sources with cardinality I^*.

In real applications, sources appear as piecewise constant images (contours of binary values) which implies compact sparse/ compressible representations in wavelet domain for both S^i and X^j. We define matrix Σ to be the 2D wavelet coefficients of the rows of S and from the model (3) we can deduce

$$X = A_{\mathcal{I}^*} \Sigma_{\mathcal{I}^*} \Psi^T, \tag{4}$$

where, Ψ is the 2D wavelet basis.

In the next sections we take this representation of the hyperspectral images which contains both sparsification along slices (due to the wavelet transform) and dimension reduction from J to I^* (thanks to the few existing sources), to develop a coding/decoding scheme that compress the whole cubic image in few number of measurements to be sampled and transmitted.

2.2. Sampling and Transmission Mechanism

In this section we describe our compression scheme which merges the idea of compressed sampling together with utilizing the knowledge of the mixture model $X = AS$, in order to efficiently reduce the number of the samples and transmitted data. Note that, we need to know what are the materials that can be present in the HSI as well as their spectral response which can be picked out of a spectral library like the USGS digital spectral library [8]. More details are as follows:

- For each spectral channel j, we sample its corresponding image by only $M < N$ linear measurements

$$(Y^j)^T = \Phi(X^j)^T, \tag{5}$$

where, $\Phi \in \mathbb{R}^{M \times N}$ is the *sampling matrix* which is unique for all channels, and we choose it to be i.i.d. random Gaus-

sian due to nice properties [1] of these types of matrices for compression. In HSI applications, Φ can be implemented by flipping the micromirrors of DMD at random. Stacking these samples together we form the $J \times M$ matrix of measurements $Y = X\Phi^T$.

- We apply the pseudo inverse matrix $A^\dagger = (A^T A)^{-1} A^T$ from the left side to Y and threshold out the rows with zero energy to have only measurements from the active sources. Considering the model (4) for the observations, this step results in dimension reduction of Y to a $I^* \times M$ matrix as following,

$$\overline{Y} = [A^\dagger Y]_+ = \Sigma_{\mathcal{I}^*} \Psi^T \Phi^T. \tag{6}$$

Here, by $[.]_+$ we denote the thresholding operator that applies on matrices to pick their rows with nonzero energy.

Following the steps above, finally we transmit the indices of the active sources $\mathcal{I}^*$ plus their compressed measurements to the base station and what is received is typically corrupted by some noise (e.g. quantization, transmission noise and mismatch with model (2) due to some unexpected material frequency response) which can be modeled by,

$$\widetilde{Y} = \Sigma_{\mathcal{I}^*} \Psi^T \Phi^T + Z. \tag{7}$$

$Z \in \mathbb{R}^{I^* \times M}$ is the noise matrix that is assumed to have elements with i.i.d. $\mathcal{N}(0, \sigma^2)$ distribution.

Note that, to be able to define $A^\dagger$ in the second step, A has to be a full rank matrix. Having a fix number of channels, this fact obviously pose an upper bound on the number of sources to be detected such that, at least $I \leq J$. In addition, if observations do not perfectly obey the model 2 (e.g., due to some noise), in order to have stability, A has to be chosen such that its pseudo inverse prevents a huge amplification of noise, which implies even further constraints (roughly saying it results in $I \ll J$). Note that, in the case where A would be close to be singular, it would be still possible to use the *regularized pseudo-inverse* operator $(A^T A + \epsilon I)^{-1} A^T$, where ϵ is a small number. We also need to update the thresholding operator to pick rows of $A^\dagger Y$, containing more than a certain level of energy.

3. MULTICHANNEL RECOVERY ALGORITHM

In this section we describe our algorithm which recovers the multichannel data X from a set of incomplete noisy measurements $\widetilde{Y}$. The measurement matrix Φ has to be known at the base station. As previously mentioned, the main feature of our scheme lies in recovering the independent sources S, rather than estimating directly the multichannel data. For this purpose let us rewrite (7) as,

$$\mathbf{Vec}(\widetilde{Y}) = \tilde{\mathbf{\Phi}} \mathbf{Vec}(\Sigma_{\mathcal{I}^*}) + \mathbf{Vec}(Z). \tag{8}$$

Where, $\mathbf{Vec}(.)$ reshapes the columns of a matrix to a vector and bold face $\tilde{\mathbf{\Phi}} \in \mathbb{R}^{MI^* \times NI^*}$ is the Kronecker product between the $I^* \times I^*$ identity matrix and $\Phi\Psi$ i,e., $\tilde{\mathbf{\Phi}} = \Phi\Psi \otimes \mathbf{Id}_{I^*}$.

Considering the fact that sources have sparse representations in wavelet domain, the source recovery problem can be formulated as the solution to the following non-convex optimization,

$$\widehat{\Sigma}_{\mathcal{I}^*} = \underset{\widetilde{\Sigma}_{\mathcal{I}^*} \in \mathcal{B}}{\arg\min} \|\mathbf{Vec}(\widetilde{\Sigma}_{\mathcal{I}^*})\|_0$$
$$s.t. \quad \|\mathbf{Vec}(\widetilde{Y}) - \tilde{\mathbf{\Phi}} \mathbf{Vec}(\widetilde{\Sigma}_{\mathcal{I}^*})\|_2 \leq \epsilon \tag{9}$$

---

[1] Random Gaussian matrices have the property of being low-coherent with any orthogonal basis, with a very high probability [3, 2, 4, 5].

(a) Original data.

(b) Reconstruction without the thresholding step (Normalized MSE=0.23).

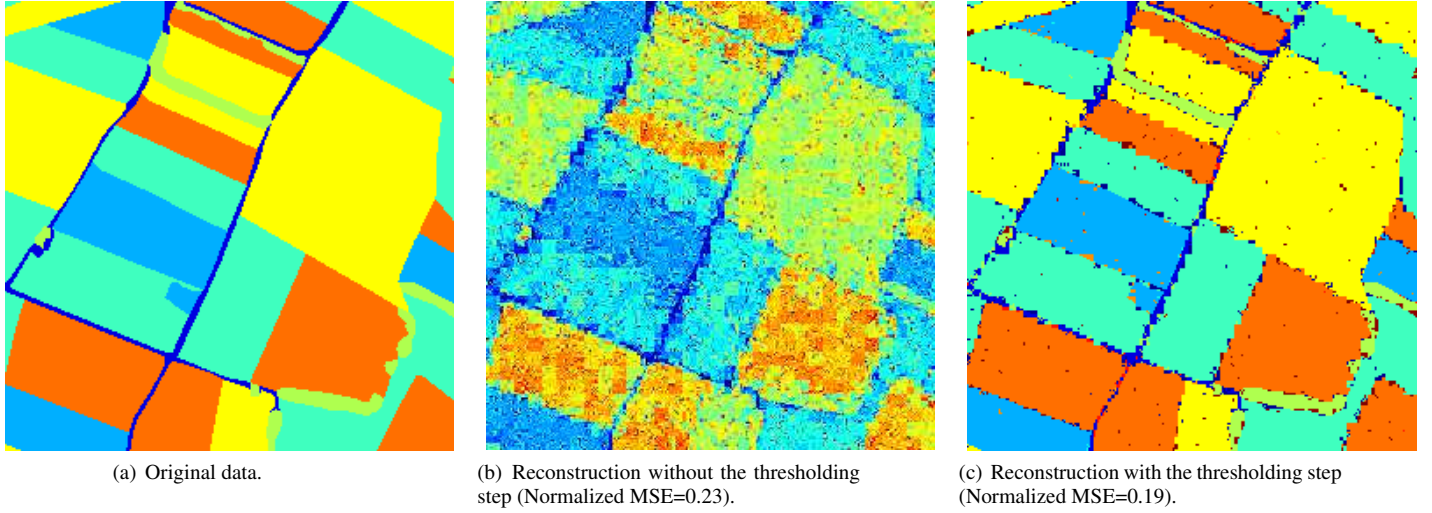(c) Reconstruction with the thresholding step (Normalized MSE=0.19).

Fig. 1. Reconstruction of HSI using our recovery scheme, by randomly sampling 0.45% of the original cube, demonstrated for a slice/channel $j = 90$.

Here, l_0-norm counts the number of the nonzero elements in a vector, and $\mathcal{B}$ denotes the set of matrices such that the inverse wavelet transform of its rows (i.e. rows of the matrix $\widetilde{\Sigma}_{\mathcal{I}^*} \Psi^T$) have binary elements, and are disjoints with each other. This optimization uniquely recovers $\mathbf{Vec}(\Sigma_{\mathcal{I}^*})$ if it is sparse enough, however, finding this solution is NP-hard [9].

To have a feasible solution which estimates (9) with a polynomial-time algorithm, our scheme proposes the two following steps:

- First, by using the idea of [2, 3] we substitute the l_0 minimization by l_1, i.e.,

$$\widehat{\Sigma}_{\mathcal{I}^*} = \arg\min \|\mathbf{Vec}(\widetilde{\Sigma}_{\mathcal{I}^*})\|_1$$
$$s.t. \quad \|\mathbf{Vec}(\widetilde{Y}) - \widetilde{\mathbf{\Phi}} \, \mathbf{Vec}(\widetilde{\Sigma}_{\mathcal{I}^*})\|_2 \leq \epsilon \quad (10)$$

  This minimization can be solved via *second-order cone program* (SOCP) with a polynomial time complexity. However, the solutions obviously may not belong to the set $\mathcal{B}$.

- In order to reconstruct sources that follow our model, here, we add a simple thresholding step to refine the solution of $l1$-minimization. More precisely, after recovering $\widehat{\Sigma}_{\mathcal{I}^*}$ from (10), we apply the inverse wavelet transform to find $\widehat{S}_{\mathcal{I}^*}$. Now, since each pixel of the image can only belong to one source, for each column of $\widehat{S}_{\mathcal{I}^*}$, we set the value of its largest element to one and the rest to zero. In this way, we associate each pixel to the source that is most likely to be belonged to.

Once the algorithm determines the sources, the whole HSI cube can be recovered through the mixing model in (3).

4. SIMULATIONS AND PERFORMANCE ANALYSIS

Our simulations are based on HSI synthesized using (2), where $I^* = 6$ sources are extracted from a ground truth map image[2] of farms at the suburb of Geneva city and the source spectra (i.e. matrix A) are choosen at random form the USGS digital spectral library [3] [8].
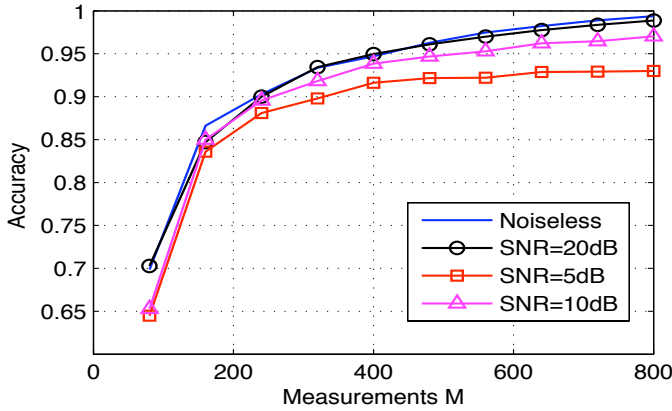
---

[2] We acknowledge Xavier Gigandet for providing this ground truth map.
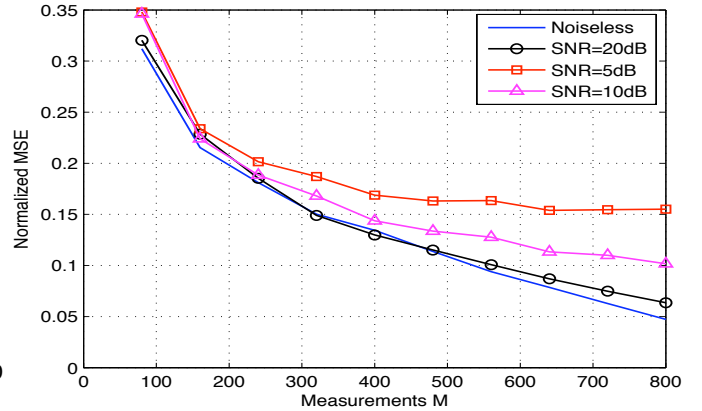[3] Available at the url http://speclab.cr.usgs.gov/spectral.lib06.

Figure 1(a) shows one channel of the resulting HSI. The HSI cube consists of dimension $256 \times 256 \times 128$, which indicates slices of the resolution $N = 256 \times 256$ that are taken over $J = 128$ frequency bands. The encoder (e.g. satellite) assumed to be provided by the knowledge of the materials (i.e. matrix A) that are potentially existing in the region (here $I = 36$, including the true existing source spectra). Following our sampling scheme, we set $M = 6400$ to randomly sample the whole cube by about 10% of its original size. Further, we apply the decorrelation step and we transmit only MI^* measurements (i.e., about 0.45% of the original HSI) to the base station. Figure 1 compares the recovery performance of our algorithm for one slice of the HSI, with and without applying the thresholding step. As we can see, applying thresholding decreases MSE only by 4%, however, comparing those images, 1(c) looks much more similar to the original one. This highlights the role of source separation by the last thresholding step, which results in recovering images that are piecewise constant and indeed looking more natural.

In the second setup we choose the first 64×64 pixels of the upper left part of the images across the first 64 spectral channels, which enables us to run quick experiments that evaluates the average performance of our scheme for various compression matrices of different sizes. Figures 2(a) and 2(b) respectively demonstrate the accuracy — that is the ratio of the misclassified pixels to the total number of pixels in the source image — of the source separation and the reconstruction error, under different SNR regimes and for different compression sizes. The plots are averaged over 20 independent realizations of the random measurement matrix and Gaussian additive noise. Both figures indicate stable recovery, improving by increasing M, up to a limit that is determined by the noise power. It is noteworthy that, the total number of measurements has to be transmitted to have an acceptable reconstruction (say, with accuracy $> 90\%$) is only about 0.34% of the size of the original HSI.

Figure 3 compares the performance of the classical CS scheme applied on each channel separately (i.e., compression/reconstruction of each slice of HSI independently) with the one of our CS scheme via source separation (Source CS). As we can observe, thanks to exploiting the underlying correlations in HSI, our scheme indicates a huge gain in reconstruction for a fixed M. Moreover, comparing

(a) Source separation accuracy vs number of measurements.

(b) Reconstruction Normalized MSE vs number of measurements.

Fig. 2. Source separation accuracy and HSI reconstruction error (normalized MSE) of our recovery scheme, for different levels of noise and different number of measurements M.
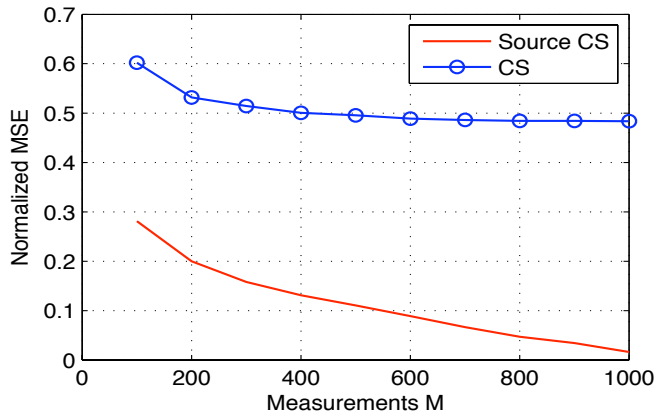

Fig. 3. Reconstruction error of the HSI (Normalized MSE) using classical CS recovery (applied separately on each channel), and our source separation based recovery scheme (Source CS).

to the classical CS, this improvement is achieved by transmitting only MI^* measurements (instead of MJ), which significantly saves the battery life of the satellite and the complexity of the decoding algorithm.

5. CONCLUSION

In this paper, we proposed a new method for compressive sampling (CS) of multichannel data which exploits the correlation across the channels via a source mixture model. Based on the knowledge of the mixture parameters, we apply a decorrelation step, so that the number of the measurements to be transmitted scales with the number of the sources. Since the source images have sparse representations in 2D wavelet basis, at the decoder side, we solve an inverse problem with relaxed sparsity constraint (l_1-minimization), which follows by a thresholding step to reconstruct the sources (hence, the whole data) from those few measurements. We run several simulations on hyperspectral images indicating that our scheme stably recovers the noisy multichannel data and it outperforms the classical CS scheme which recovers data of each channel separately. However, one of the main

limitation of this approach is that the spectral response of the materials of the HSI, i.e. the matrix A, has to be known in advance. Future works include the estimation or re-estimation of the spectral matrix A so as to deal with situations where the materials which compose the HSI are unknown or different from the spectral library.

6. REFERENCES

[1] Jing Wang and Chein-I Chang, "Independent component analysis-based dimensionality reduction with applications in hyperspectral image analysis," *Geoscience and Remote Sensing, IEEE Transactions on DOI - 10.1109/TGRS.2005.863297*, vol. 44, no. 6, pp. 1586– 1600, 2006.

[2] E.J. Candes, "The restricted isometry property and its implications for compressed sensing," *Comptes rendus-Mathématique*, vol. 346, no. 9-10, pp. 589–592, 2008.

[3] D.L. Donoho, "Compressed sensing," *IEEE Transactions on Information Theory*, vol. 52, no. 4, pp. 1289–1306, 2006.

[4] M.F. Duarte, M.A. Davenport, D. Takhar, J.N. Laska, T. Sun, K.F. Kelly, and R.G. Baraniuk, "Single-pixel imaging via compressive sampling," *IEEE Signal Processing Magazine*, vol. 25, no. 2, pp. 83–91, 2008.

[5] M.F. Duarte and R.G. Baraniuk, "Kronecker Compressive Sensing," *Submitted to IEEE Transactions on Image Processing*, 2009.

[6] M.F. Duarte, S. Sarvotham, D. Baron, M.B. Wakin, and R.G. Baraniuk, "Distributed compressed sensing of jointly sparse signals," in *Asilomar Conf. Signals, Sys., Comput*, 2005, pp. 1537–1541.

[7] Y.C. Eldar, P. Kuppinger, and H. Bölcskei, "Compressed sensing of block-sparse signals: Uncertainty relations and efficient recovery," *Arxiv preprint arXiv:0906.3173, submitted to IEEE Transactions on Signal Processing*, 2009.

[8] RN Clark, GA Swayze, R. Wise, E. Livo, T. Hoefen, R. Kokaly, and SJ Sutley, "USGS digital spectral library splib06a," *US Geological Survey, Data Series*, vol. 231, 2007.

[9] B. Natarajan, "Sparse approximate solutions to linear systems," *SIAM Journal on Computing*, vol. 24, pp. 227, 1995.